

# TAP: The Attention Patch for Cross-Modal Knowledge Transfer from Unlabeled Data

Yinsong Wang<sup>1</sup> Shahin Shahrampour<sup>1</sup>

## Abstract

This work investigates the intersection of cross-modal learning and semi-supervised learning, where we aim to improve the supervised learning performance of the primary modality by borrowing missing information from an unlabeled modality. We investigate this problem from a Nadaraya–Watson (NW) kernel regression perspective and show that this formulation implicitly leads to a kernelized cross-attention module. To this end, we propose The Attention Patch (TAP), a simple neural network plugin that allows data-level knowledge transfer from the unlabeled modality. We provide numerical simulations on three real-world datasets to examine each aspect of TAP and show that a TAP integration in a neural network can improve generalization performance using the unlabeled modality.

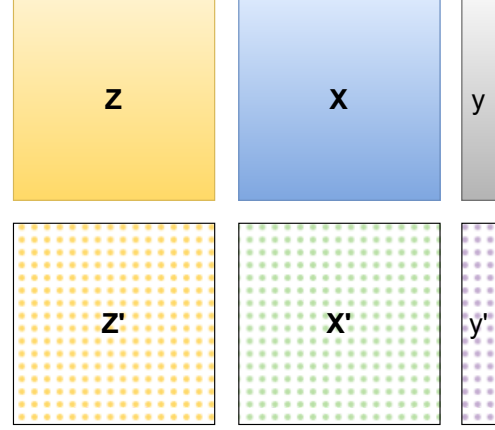


Figure 1. Visualization of data structure.  $\mathbf{X}, \mathbf{X}' \in \mathcal{X}$  and  $\mathbf{Z}, \mathbf{Z}' \in \mathcal{Z}$  are data from different modalities.  $\mathbf{y}, \mathbf{y}' \in \mathcal{Y}$  are the corresponding labels.

## 1. Introduction

In supervised learning, the difference between various learning frameworks can be defined by the data availability at the learning stage using the data partition in Fig. 1. For example, cross-modal learning aims at combining complementary information from two input sources to improve learning tasks. With the advancements in data collection and deep learning, cross-modal learning has become more prevalent in different communities. The general consensus is that data from different modalities, like data matrix  $\mathbf{Z}$  and  $\mathbf{X}$  in Fig. 1, often contain “extra” information with respect to each other that one can make use of. This consensus has inspired different branches of cross-modal learning, including cross-modal retrieval (Wang et al., 2016), cross-modal generative learning (Gu et al., 2018; Peng & Qi, 2019), and cross-modal supervised learning (Castellano et al., 2008; Gehler & Nowozin, 2009; Ramirez et al., 2011; Bucak et al., 2013). Specifically, cross-modal supervised learning focuses on learning the function mapping  $f : \mathcal{X} \times \mathcal{Z} \rightarrow \mathcal{Y}$

using cross-modal input  $\mathbf{X}$  and  $\mathbf{Z}$  and their corresponding labels  $\mathbf{y}$ .

Despite the difference in focus, the general framework of cross-modal learning is often the same. Given a pair of cross-modal inputs, one should devise a model or learning algorithm for finding shared information, complementary information, or a latent space that can describe both modalities based on the matching pair information. The general cross-modal learning framework relies on the alignment or weak alignment (sequence input) between modalities  $\mathbf{X}$  and  $\mathbf{Z}$  to learn anything meaningful. Furthermore, most cross-modal learning algorithms need both modalities as input at the time of evaluation.

The existence of alignment between modalities in the field of cross-modal learning has never been a major concern in research works. However, it is not hard to imagine that there are cases when one would know that a modality contains “extra” information for a specific task, but it cannot be used in the learning process due to reasons like expensive labeling costs, or the dataset is sampled at a different time and space comparing to the primary dataset used for this learning task.

On the other hand, the area of semi-supervised learning has been solely focusing on utilizing unlabeled “extra” infor-

<sup>1</sup>Department of Mechanical and Industrial Engineering, Northeastern University, Boston, United States. Correspondence to: Yinsong Wang <wang.yinso@northeastern.edu>.

mation. The motivation behind semi-supervised learning is mainly the limited availability of labeled data. Thus, different approaches have been devised for the purpose of utilizing unlabeled data to improve the learning objective. That is, learning a function  $f : \mathcal{X} \rightarrow \mathcal{Y}$  using labeled data pairs  $\mathbf{X}, \mathbf{y}$  and unlabeled data  $\mathbf{X}'$  (Fig. 1). There also exists literature that studies the case where the full dataset, both labeled and unlabeled, is cross-modal (Zhang et al., 2017; Yu et al., 2018; Liang et al., 2020; Hong et al., 2020; Zhang et al., 2021), i.e.,  $\mathbf{X}, \mathbf{Z}, \mathbf{y}, \mathbf{X}', \mathbf{Z}'$  are *all* available during the learning stage.

However, there is no study for the case where only  $\mathbf{X}, \mathbf{y}, \mathbf{Z}'$  are available during the learning process, which is the main motivation of this work.

### 1.1. Contribution

- This is the first work, to the best of our knowledge, that investigates the intersection of cross-modal supervised learning and semi-supervised learning, where the “extra” information  $\mathbf{Z}'$  is not only unlabeled and unpaired but also comes from a different modality than the limited primary data  $\mathbf{X}$ .
- In Section 3, we propose the Nadaraya-Watson (NW) kernel regression formulation of missing information estimation using unlabeled cross-modal data. Borrowing two well-known techniques in cross-modal learning and semi-supervised learning, we show that this formulation recovers a kernelized version of the popular *cross-attention* mechanism (Vaswani et al., 2017).
- Based on our observation, we propose The Attention Patch (TAP) neural network plugin for cross-modal knowledge transfer from unlabeled modality. We show that the NW kernel regression formulation yields an asymptotically vanishing error. We further propose a batch training strategy from a practical standpoint.
- We provide detailed simulations on three real-world datasets to examine each aspect of TAP and show a TAP integration in a neural network can improve generalization performance using the unlabeled modality.

## 2. Related Literature

### 2.1. Cross-Modal Learning

Cross-modal learning focuses on learning with data from different modalities. The most representative topic application-wise is cross-modal retrieval. This topic focuses on finding relevant samples in one modality given a query in another modality (Wang et al., 2016). The most important step in cross-modal retrieval tasks is learning a coupled space that can correctly describe the correlation between data points from different modalities. Traditional techniques including

canonical correlation analysis (Hardoon et al., 2004; Andrew et al., 2013; Wang & Shahrampour, 2021), partial least squares (Geladi & Kowalski, 1986; Cha, 1994), and bilinear model (Sharma et al., 2012; Tenenbaum & Freeman, 2000) find a simple projection of the matching pairs that minimizes certain pre-defined loss function. This framework, though have seen several variants and extensions (Ngiam et al., 2011; Hong et al., 2015; Sohn et al., 2014; Xu et al., 2015), remains the most popular framework in cross-modal correlation learning.

In addition to cross-modal retrieval, cross-modal supervised learning also follows the same principle. Examples include but are not limited to (Lin & Tang, 2006; Evangelopoulos et al., 2013; Jing et al., 2014; Feichtenhofer et al., 2016; Peng et al., 2017; Li et al., 2019). All of these models involve coupled space learning through either implicit or explicit learning loss with matching pairs of cross-modal inputs.

With the rise in popularity of natural language processing and time series analysis, a new concept of weak alignment appears in cross-modal learning. Weak alignment refers to the missing alignment of sub-components in instances from different modalities (Baltrušaitis et al., 2018). More specifically, this often means cross-modal input sequences with different sampling intervals or orders. For example, in the case of vision and language models, a text description sequence of a video will usually differ from the time and order of information that appeared in the video (Venugopalan et al., 2015; Tsai et al., 2019), or a text description of an image will need to map a sequence of words to a collection of objects without any specific orders (Mitchell et al., 2012; Kulkarni et al., 2013; Chen et al., 2015; Karpathy & Fei-Fei, 2015).

There exists a research direction that taps into instance-wise unalignment for cross-modal learning, which is called non-parallel co-learning (Baltrušaitis et al., 2018). Non-parallel co-learning aims at improving the model learned on a single modality using another modality that is unaligned with the primary data. However, this is a concept that has only been studied with very specific applications, and it also requires the reference modality to be labeled during the training process. For example, cross-modal transfer learning (Frome et al., 2013; Kiela & Bottou, 2014; Mahasseni & Todorovic, 2016) mainly focuses on transferring supervised pre-trained embedding networks for improved cross-model prediction accuracy.

In a nutshell, almost all cross-modal learning frameworks focus on the case where there are known alignments between different modalities of data at least during the learning phase. Our work considers the case where both alignment and labels do not exist during learning, and our proposed architecture can be applied to arbitrary modalities.

## 2.2. Semi-Supervised Learning

Semi-supervised learning focuses on addressing the challenge of limited labeled data availability in building a learning algorithm (Zhu, 2005; Van Engelen & Hoos, 2020). Among all kinds of semi-supervised learning methods, self-training is the closest class of methods that relates to our study. Self-training refers to the class of methods that train a supervised learning algorithm using labeled and unlabeled data together (Triguero et al., 2015). This approach is usually done by assigning pseudo labels to the unlabeled data, and jointly refining the supervised learning model and the pseudo labels by iterative training (Yarowsky, 1995; Rosenberg et al., 2005; Dópido et al., 2013; Wu et al., 2012; Tanha et al., 2017). For most traditional learners, this means re-training the learning algorithm many times as the pseudo labels are being updated. However, this pseudo-label training approach naturally works with incremental learning algorithms like neural networks, where the model is gradually learned through optimizing an objective function (Lee et al., 2013; Berthelot et al., 2019; Zoph et al., 2020; Xie et al., 2020; Sohn et al., 2020). Strictly speaking, all pseudo-labeling/self-training methods focus on assigning labels in the prediction space to the data points in the primary space that is the same as the labeled data.

There exists another line of research that studies semi-supervised learning in the context of multi-view or multi-modal learning. For example, multi-view co-training (Blum & Mitchell, 1998; Kiritchenko & Matwin, 2001; Wan, 2009; Du et al., 2010) propose to train different classifiers on different views of the same data. Multi-view co-training generally assumes the two views are independent of each other but can perform equally well in a single-view prediction task. The development of deep neural networks also introduced a lot of cross-modal semi-supervised learning works, which mainly focus on computer vision and natural language processing (Nie et al., 2017b;a; 2019; Jia et al., 2020). Again, all of these mentioned works rely on the availability of labels in all the modalities.

As we can see, all existing semi-supervised learning frameworks consider the case where the unlabeled data resides in the same space or joint space as the labeled data. Our work considers the case where the unlabeled data resides in a completely different space than the labeled data.

## 3. Estimating the Missing Information

As discussed in the Introduction (Fig. 1), we are concerned with knowledge transfer from unlabeled modality  $\mathbf{Z}' \in \mathbb{R}^{n'_z \times d_z}$  for improved generalization. That is, to devise a framework to extract the missing information of  $\mathbf{X}$  that is contained in  $\mathbf{Z}'$ . To this end, we first define two *latent* spaces  $\mathcal{M}^1$  and  $\mathcal{M}^2$ , where a mapping  $\phi_1 : \mathcal{Z} \rightarrow \mathcal{M}^1$  extracts the

shared information between  $\mathcal{Z}$  and  $\mathcal{X}$ , and  $\phi_2 : \mathcal{Z} \rightarrow \mathcal{M}^2$  extracts the exclusive information in  $\mathcal{Z}$  that is not present in  $\mathcal{X}$ .

In this section, we start by investigating the missing information estimation, specifically  $\mathbb{E}(\phi_2(\mathbf{z})|\mathbf{x})$ , from the Nadaraya-Watson kernel regression perspective and we formulate it using unlabeled reference  $\mathbf{Z}'$ . Then, we identify two major challenges under this formulation (Remark 3.1) and show how we can potentially solve them using two well-known techniques in cross-modal learning and semi-supervised learning. Finally, we show that the entire estimation process recovers a kernelized *cross-attention* formulation in (6).

### 3.1. Nadaraya-Watson Kernel Regression

We first write the conditional expectation as its standard definition

$$\mathbb{E}(\phi_2(\mathbf{z})|\mathbf{x}) = \int \phi_2(\mathbf{z}) \frac{p_1(\phi_2(\mathbf{z}), \mathbf{x})}{p_2(\mathbf{x})} d\phi_2(\mathbf{z}), \quad (1)$$

where  $p_1(\phi_2(\mathbf{z}), \mathbf{x})$  is the joint density of  $\phi_2(\mathbf{z})$  and  $\mathbf{x}$ , and  $p_2(\mathbf{x})$  is the marginal density of  $\mathbf{x}$ .

To bring in the information contained in the unlabeled data modality  $\mathbf{Z}' \in \mathbb{R}^{n'_z \times d_z}$ , we carry out the kernel density estimations using solely instances  $\mathbf{z}'_i$  ( $i$ -th row of  $\mathbf{Z}'$ ) as the reference points. By defining a generalized kernel density function  $g(\cdot, \cdot)$  that can describe the correlation of an input pair from two modalities with shared information, we have the following

$$\begin{aligned} p_1(\phi_2(\mathbf{z}), \mathbf{x}) &\approx \frac{1}{n'_z} \sum_{i=1}^{n'_z} g(\mathbf{x}, \phi_1(\mathbf{z}'_i)) k_0(\phi_2(\mathbf{z}), \phi_2(\mathbf{z}'_i)) \\ &\triangleq \hat{p}_1(\phi_2(\mathbf{z}), \mathbf{x}) \\ p_2(\mathbf{x}) &\approx \frac{1}{n'_z} \sum_{i=1}^{n'_z} g(\mathbf{x}, \phi_1(\mathbf{z}'_i)) \triangleq \hat{p}_2(\mathbf{x}), \end{aligned} \quad (2)$$

where  $k_0$  can be a standard kernel function with inputs from the same modality. In an ideal situation, the first expression should be in terms of  $k(\mathbf{x}, \mathbf{x}'_i) k_0(\phi_2(\mathbf{z}), \phi_2(\mathbf{z}'_i))$  for some standard kernel functions  $k$  and  $k_0$ , where  $\mathbf{x}'_i$  is the  $i$ -th row of  $\mathbf{X}'$ . However, since  $\mathbf{X}'$  is not available, we can not use this approach.

Next, plugging the above density estimations back into (1),

we have the following

$$\begin{aligned}
 & \mathbb{E}(\phi_2(\mathbf{z})|\mathbf{x}) \\
 & \approx \int \phi_2(\mathbf{z}) \frac{\hat{p}_1(\phi_2(\mathbf{z}), \mathbf{x})}{\hat{p}_2(\mathbf{x})} d\phi_2(\mathbf{z}) \\
 & \approx \sum_{i=1}^{n'_z} \frac{\int \phi_2(\mathbf{z}) g(\mathbf{x}, \phi_1(\mathbf{z}'_i)) k_0(\phi_2(\mathbf{z}), \phi_2(\mathbf{z}'_i)) d\phi_2(\mathbf{z})}{\sum_{j=1}^{n'_z} g(\mathbf{x}, \phi_1(\mathbf{z}'_j))} \\
 & = \sum_{i=1}^{n'_z} \frac{g(\mathbf{x}, \phi_1(\mathbf{z}'_i)) \int \phi_2(\mathbf{z}) k_0(\phi_2(\mathbf{z}), \phi_2(\mathbf{z}'_i)) d\phi_2(\mathbf{z})}{\sum_{j=1}^{n'_z} g(\mathbf{x}, \phi_1(\mathbf{z}'_j))}. \tag{3}
 \end{aligned}$$

We now investigate the relation between (3) and the well-known Nadaraya-Watson kernel regression estimator (Nadaraya, 1964; Watson, 1964). In the context of missing information estimation, the exact formulation of NW kernel regression is as follows

$$\mathbb{E}(\phi_2(\mathbf{z})|\mathbf{x}) \approx \sum_{i=1}^{n'_z} \frac{k(\mathbf{x}, \mathbf{x}'_i) \phi_2(\mathbf{z}'_i)}{\sum_{j=1}^{n'_z} k(\mathbf{x}, \mathbf{x}'_j)}, \tag{4}$$

where the matching pairs  $\mathbf{x}'_i$  and  $\mathbf{z}'_i$  are available. Note that the above formulation is identical to (3) when  $g(\mathbf{x}, \phi_1(\mathbf{z}'_i)) = k(\mathbf{x}, \mathbf{x}'_i)$ , and  $\int \phi_2(\mathbf{z}) k_0(\phi_2(\mathbf{z}), \phi_2(\mathbf{z}'_i)) d\phi_2(\mathbf{z}) = \phi_2(\mathbf{z}'_i)$ , where the latter is true for several shift-invariant kernels, such as the Gaussian kernel. Basically, this is satisfied for any kernel  $k_0(\cdot - \mu)$  that is a density function with a mean  $\mu$ .

*Remark 3.1.* To account for the missing modality  $\mathbf{X}'$  in the NW kernel regression, we need to introduce the generalized kernel function  $g$  that takes input from two different modalities. This implies the reference modality  $\mathbf{Z}'$  needs to be information-rich, such that it shares information with  $\mathbf{X}$  for correlation calculation in addition to the “extra” information that  $\mathbf{X}$  does not have. However, there are still two major challenges that prohibit using (3) to estimate the missing information:

1. How do we define the generalized kernel function  $g$ , such that it is a proper kernel density function that works on cross-modal inputs?
2. How do we find the mapping  $\phi_2 : \mathcal{Z} \rightarrow \mathcal{M}^2$ ?

### 3.2. Neural Network Integration

To address the challenges mentioned in Remark 3.1, we propose a direct neural network integration of (3), so that the learning process can be done implicitly. In fact, a neural network integration allows us to define a pair of transformations  $\phi_3 : \mathcal{X} \rightarrow \mathcal{M}^1$  and  $\phi_1 : \mathcal{Z} \rightarrow \mathcal{M}^1$  that transform  $\mathbf{x}$  and  $\mathbf{z}$  to the same space  $\mathcal{M}^1$  for correlation calculation. In this case, we can recover the exact NW kernel regression

estimator

$$\mathbb{E}(\phi_2(\mathbf{z})|\phi_3(\mathbf{x})) \approx \sum_{i=1}^{n'_z} \frac{k(\phi_3(\mathbf{x}), \phi_1(\mathbf{z}'_i)) \phi_2(\mathbf{z}'_i)}{\sum_{j=1}^{n'_z} k(\phi_3(\mathbf{x}), \phi_1(\mathbf{z}'_j))}. \tag{5}$$

The transformations  $\phi_3$  and  $\phi_1$  can be simply defined with trainable linear transformation matrices  $\phi_3(\mathbf{x}) \approx \mathbf{W}_q \mathbf{x}$  and  $\phi_1(\mathbf{z}'_i) \approx \mathbf{W}_k \mathbf{z}'_i$ . This workaround is identical to cross-modal correlation learning as mentioned in Section 2.

On the other hand, finding the missing information in  $\mathcal{M}^2$  requires learning the transformation  $\phi_2$ . This can also be made possible with pseudo-labeling techniques, where we iteratively refine the pseudo-labels throughout network training. Since we know the representation is only dependent on  $\mathbf{z}'_i$ , we can approximate the labeling logic with another trainable linear transformation  $\phi_2(\mathbf{z}'_i) \approx \mathbf{W}_v \mathbf{z}'_i$ .

Putting together all of these transformations, we have the following expression

$$\mathbb{E}(\phi_2(\mathbf{z})|\phi_3(\mathbf{x})) \approx \sum_{i=1}^{n'_z} \frac{k(\mathbf{W}_q \mathbf{x}, \mathbf{W}_k \mathbf{z}'_i) \mathbf{W}_v \mathbf{z}'_i}{\sum_{j=1}^{n'_z} k(\mathbf{W}_q \mathbf{x}, \mathbf{W}_k \mathbf{z}'_j)}, \tag{6}$$

where the RHS becomes the popular kernelized cross-attention module.

The above formulation shows that at any point in a neural network, we can potentially feed in unlabeled reference data points  $\mathbf{Z}' \in \mathbb{R}^{n'_z \times d_z}$  from a different modality to extract useful information from the seemingly unusable data. This reference mechanism is approximately equivalent to a cross-attention module with keys and values  $\mathbf{Z}'$  of sequence length  $n'_z$  and dimension  $d_z$  (before transformation).

*Remark 3.2.* The neural network integration of NW kernel regression ultimately employs two approaches in the fields of cross-modal and semi-supervised learning. First, a similarity measure  $g$  between two modalities is defined after a latent space transformation, similar to the class of correlation learning methods we mentioned in Section 2. Second, the approximation of the integral term can be viewed as a multi-dimensional pseudo-labeling approach, which will be iteratively updated during neural network training. Everything will be learned implicitly during network training just like self-training.

## 4. The Attention Patch

In this section, we will formally define The Attention Patch (TAP) neural network plugin. We will first introduce the reasons behind the kernelization of TAP following NW kernel regression by showing the estimation error asymptotically goes to zero (Theorem 4.3), and then we will propose a batch training strategy from a practical standpoint.



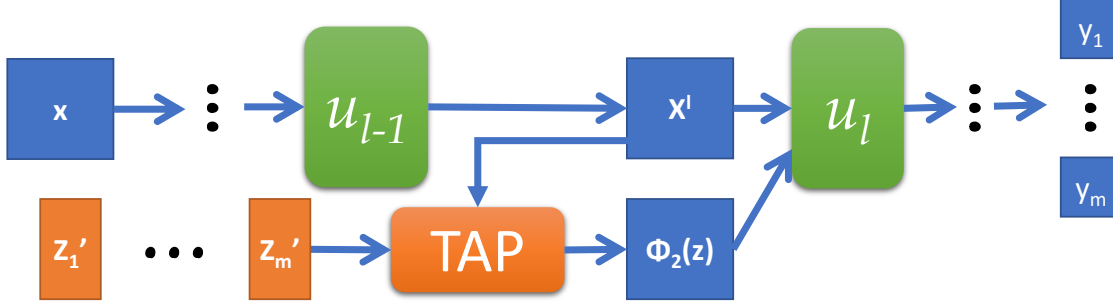


Figure 2. The Attention Patch (TAP) neural network integration visualization. TAP takes in the output  $\mathbf{x}^{l-1}$  of layer  $u_{l-1}$  to calculate the missing representation  $\phi_2(\mathbf{z})$  using a batch of reference data  $\mathbf{Z}'_i$ ,  $\phi_2(\mathbf{z})$  will be concatenated with  $\mathbf{x}^{l-1}$  to feed to the next layer, and the neural network yields a corresponding output  $y_i$  with respect to  $\mathbf{Z}'_i$ .

#### 4.1. Kernelization

Under the view of NW kernel regression, we see that the plug-in module is approximately a cross-attention module. Furthermore, we note that the formulation in the RHS of (6) extends the popular dot-product attention proposed in (Vaswani et al., 2017) to a class of kernelized attention. Although there is no study investigating the attention mechanism from an NW kernel regression perspective, the kernelized attention approach has appeared in several studies (Peng et al., 2020; Choromanski et al., 2020; Chen et al., 2021; Luo et al., 2021; Xiong et al., 2021). In all of these studies, the kernelization approach is raised based on the similarity between an exponential lift of dot-product in the softmax function and a Gaussian kernel function. It is also empirically shown in these studies that an actual kernel function, especially the Gaussian kernel, will generally improve the model performance and stability. However, there has been no study on why the actual kernel attention enjoys a better performance from a theoretical perspective. Here, we theoretically investigate why kernelization can be helpful from an NW kernel regression perspective.

Given that (5) is motivated by (4), we want to characterize the estimation error of the NW kernel regression estimator. Without loss of generality, we use the following generic version of the NW kernel regression in this subsection,

$$\mathbb{E}(\mathbf{z}|\mathbf{x}) \approx \hat{f}(\mathbf{x}) \triangleq \sum_{i=1}^n \frac{k_{\mathbf{H}}(\mathbf{x}, \mathbf{x}'_i) \mathbf{z}'_i}{\sum_{j=1}^n k_{\mathbf{H}}(\mathbf{x}, \mathbf{x}'_j)}, \quad (7)$$

where  $\mathbf{H} = h\mathbf{I}$  is the bandwidth matrix of the kernel function, such that  $k_{\mathbf{H}}(\mathbf{x}, \mathbf{z}) = \frac{1}{|\mathbf{H}|} k(\frac{\mathbf{x}-\mathbf{z}}{|\mathbf{H}|})$ , where  $|\mathbf{H}|$  is the determinant of  $\mathbf{H}$ . The parameter  $h$  depends on  $n$ , which we make it explicit in the next assumption but disregard it in notation throughout.

**Assumption 4.1.** (Wand & Jones, 1994) The bandwidth matrix  $\mathbf{H} = h_n\mathbf{I}$  with  $|\mathbf{H}| = h_n^d$  (the subscript  $n$  shows the dependence of  $h$  to the number of data points) has the

following properties

$$\begin{aligned} \lim_{n \rightarrow \infty} h_n &= 0 \\ \lim_{n \rightarrow \infty} n h_n^d &= \infty, \end{aligned} \quad (8)$$

which implies that the bandwidth parameter  $h_n$  decays slower than  $n^{-1/d}$  and converges to 0. The standard kernel function  $k(\cdot)$  is a bounded, symmetric probability density function with a zero first moment and a finite second moment. That is, the following properties hold

$$\begin{aligned} \int_{\mathbb{R}^d} k(\mathbf{x}) d\mathbf{x} &= 1, \quad \int_{\mathbb{R}^d} \mathbf{x} k(\mathbf{x}) d\mathbf{x} = \mathbf{0} \\ \int_{\mathbb{R}^d} \mathbf{x} \mathbf{x}^\top k(\mathbf{x}) d\mathbf{x} &= \mu_2(k) \mathbf{I}, \quad \mu_2(k) < \infty \\ \int_{\mathbb{R}^d} k^2(\mathbf{x}) d\mathbf{x} &= R(k) < \infty, \end{aligned} \quad (9)$$

where  $\mu_2(k)$  and  $R(k)$  are constants decided by the choice of kernel  $k$ .

It is easy to verify that several popular shift-invariant kernels  $k(\mathbf{x} - \mathbf{y})$  (e.g., Gaussian kernel) satisfy the above assumption with proper normalization. We will later use the Gaussian kernel in our simulations.

**Assumption 4.2.** The underlying true function  $f: \mathcal{X} \rightarrow \mathcal{Z}$  and the true density function  $p(\mathbf{x})$  satisfy the followings:

- The true density function  $p(\mathbf{x})$  is differentiable and the  $\ell_2$ -norm of its gradient is bounded.
- We have for the true function that

$$\mathbf{z} = f(\mathbf{x}) + \epsilon, \quad (10)$$

where  $\epsilon$  is an isotropic noise vector from  $\mathcal{N}(\mathbf{0}, \sigma^2 \mathbf{I})$ .

- The true function  $f(\mathbf{x})$  has a bounded gradient and Hessian in the norm sense.

**Theorem 4.3.** Under assumption 4.1 and 4.2, an NW kernel regression estimator  $\hat{f}(\mathbf{x})$  with an isotropic shift-invariant kernel of bandwidth  $\mathbf{H} = h\mathbf{I}$ , as shown in RHS of equation (7) will yield an estimation error  $\mathbf{e}(\mathbf{x}) \triangleq \hat{f}(\mathbf{x}) - f(\mathbf{x})$  that asymptotically converges in distribution as

$$\sqrt{nh^d} \left( \mathbf{e}(\mathbf{x}) - \frac{h^{2d} \mu_2(k) \Psi(\mathbf{x})}{p(\mathbf{x})} \right) \xrightarrow{d} \mathcal{N}(\mathbf{0}, \frac{R(k) \sigma^2}{p(\mathbf{x})} \mathbf{I}), \quad (11)$$

where  $\mathbf{x} \in \mathbb{R}^d$ , and the  $i$ -th entry of  $\Psi(\mathbf{x})$  is

$$\Psi^{(i)}(\mathbf{x}) = \frac{1}{2} p(\mathbf{x}) \text{Tr} \left[ \nabla^2 f^{(i)}(\mathbf{x}) \right] + \text{Tr} \left[ \nabla f^{(i)}(\mathbf{x}) \nabla p(\mathbf{x})^\top \right], \quad (12)$$

where  $\nabla^2 f^{(i)}(\mathbf{x})$  and  $\nabla f^{(i)}(\mathbf{x})$  are the Hessian and gradient of  $i$ -th entry of the true function with respect to  $\mathbf{x}$ ,  $\nabla p(\mathbf{x})$  is the gradient of the true density function, and  $\text{Tr}[\cdot]$  is the trace operator.

The proof is provided in the Appendix. The above theorem shows that with proper kernel function, the estimation error  $\mathbf{e}(\mathbf{x}) \rightarrow \mathbf{0}$  as  $n \rightarrow \infty$  under Assumptions 4.1 and 4.2. This suggests that under an ideal latent space transformation and pseudo-labeling logic, the reference mechanism can benefit from more reference data points.

## 4.2. Batch Training

The attention formulation of cross-modal learning in (6) requires setting the keys and values to be the set of unlabeled reference data points  $\mathbf{Z}'$ . Theorem 4.3 suggests that using more reference data for the model will potentially result in a lower estimation error. However, the computation complexity of the cross-attention module scales linearly with respect to the sequence length of keys and values, which is equivalent to the number of reference points  $n'_z$  in  $\mathbf{Z}' \in \mathbb{R}^{n'_z \times d_z}$ . So, it is not practical to feed all the reference points at once, mainly due to memory limitations.

Therefore, we can break the reference dataset  $\mathbf{Z}'$  into  $m$  batches  $\{\mathbf{Z}'_i\}_{i=1}^m$  and train each epoch by iterating over the set of reference batches together with input batches of primary data points. This is similar in vein to training with stochastic gradient descent.

Each batch of reference points  $\mathbf{Z}'_i$  will make the neural network yield an output in space  $\mathcal{Y}$ . Evaluating all batches  $\{\mathbf{Z}'_i\}_{i=1}^m$  will in turn yield  $m$  outputs, which can be used in different ways depending on the application, like the ensemble approach (Dietterich et al., 2002; Sagi & Rokach, 2018) in classification tasks.

## 4.3. The Attention Patch Structure

The attention patch structure is shown in Fig. 2. We assume a neural network can be decomposed into a sequence of layers  $\{u_l\}_{l=1}^L$ . The Attention Patch can be inserted

between two consecutive layers  $u_{l-1} : \mathcal{X}^{l-1} \rightarrow \mathcal{X}^l$  and  $u_l : \mathcal{X}^l \rightarrow \mathcal{X}^{l+1}$ . The Attention Patch takes the layer  $u_{l-1}$ 's output  $\mathbf{x}^l \in \mathcal{X}^l$  and a batch of reference points  $\mathbf{Z}'_i \in \mathcal{Z}$  to estimate the missing information. Then, the output of The Attention Patch  $\phi_2(\mathbf{z}) \in \mathcal{M}^2$  will be concatenated with  $\mathbf{x}^l$  to form the input for the modified layer  $u_l : \mathcal{X}^l \times \mathcal{M}^2 \rightarrow \mathcal{X}^{l+1}$ . The insertion of The Attention Patch only requires one modification to the original neural network, which is enlarging the input size of layer  $u_l$  from the original dimension to the concatenation dimension.

Before TAP integration, the neural network is learned by minimizing the following objective function

$$\min_{q_{l-1}, q_l} \mathbb{E}_{\mathbf{x}, y} [\mathcal{L}(q_l(q_{l-1}(\mathbf{x})), y)], \quad (13)$$

where  $q_{l-1}$  denotes the neural network before layer  $u_l$ , and  $q_l$  denotes the neural network starting from layer  $u_l$ . After TAP integration, the new learning objective can be viewed as

$$\min_{q_{l-1}, q_l, TAP} \mathbb{E}_{\mathbf{x}, y} \left[ \sum_{i=1}^m \mathcal{L}(q_l(q_{l-1}(\mathbf{x}), TAP(\mathbf{x}^l; \mathbf{Z}'_i)), y) \right], \quad (14)$$

where  $TAP(\mathbf{x}^l; \mathbf{Z}'_i)$  is defined as the RHS of equation (6), which is parameterized by trainable attention weights  $\mathbf{W}_q, \mathbf{W}_k, \mathbf{W}_v$  and (batches of) frozen reference data  $\mathbf{Z}'_i$ .

*Remark 4.4.* The above loss formulation shows why our proposed TAP integration has the potential to tackle the challenge of knowledge transfer from unlabeled cross-modal data. The cross-modal data points are considered parameters of the neural network rather than another input modality. This resembles the intuition behind kernel learning where all training data points are considered the functional basis in the kernel space and ultimately become the parameters of the learned function.

## 5. Numerical Experiments

In this section, we evaluate TAP by plugging it into neural network classifiers. We show the effectiveness of TAP by comparing the performance of TAP-integrated networks with other variants. The simulations are implemented on three real-world datasets in different areas. Implementation details are included in the Appendix for reproducibility.

### 5.1. Datasets

To ensure a comprehensive test on the performance of TAP integration, we select three real-world cross-modal datasets in three different areas. All datasets are open-access datasets that can be found online. A detailed dataset and preprocessing description can be found in the Appendix.

**Computer Vision:** We use the MNIST dataset (MNIST) (Deng, 2012). We crop the upper half of all images as the

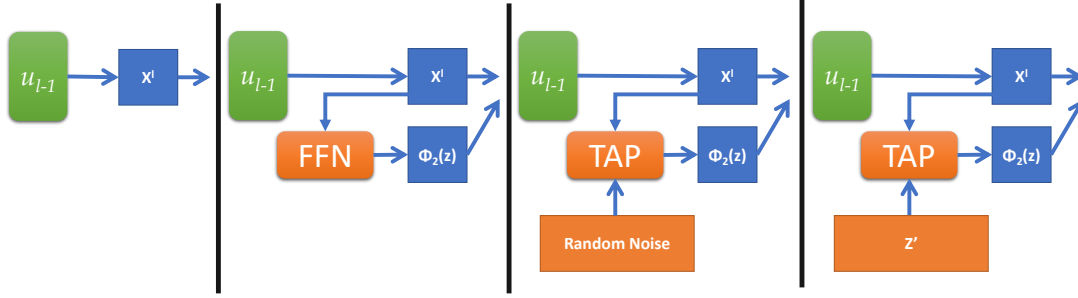


Figure 3. Benchmark models, from left to right are Baseline, FFN, Control Group, and TAP w/o Batch respectively.

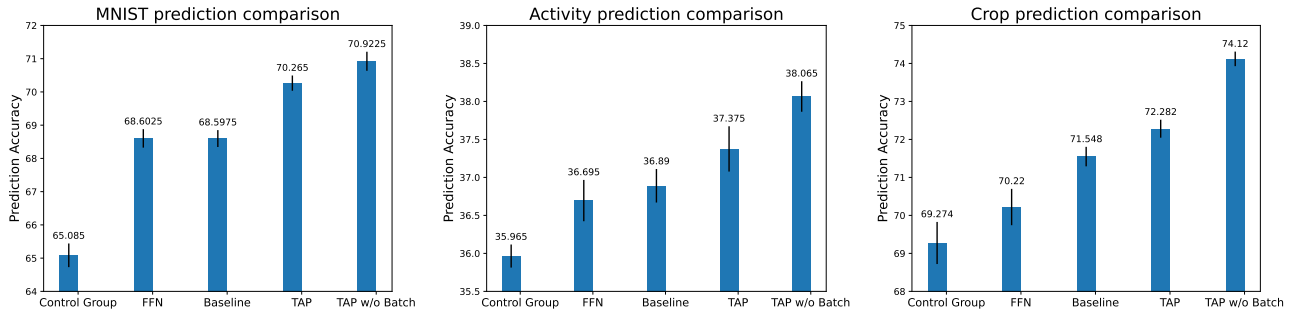


Figure 4. Simulation results on three real-world datasets. TAP integration shows a consistent performance advantage compared to other variants.

primary modal  $\mathbf{X}$  for digit prediction, and the lower half of all images as the reference modal  $\mathbf{Z}'$  (without labels).

**Healthcare:** We use the Activity dataset (Activity) (Mohino-Herranz et al., 2019). The Electrodermal Activity (EDA) signals will be the primary signal  $\mathbf{X}$  for predicting the subject activity. Thoracic Electrical Bioimpedance (TEB) signals are used as the reference dataset  $\mathbf{Z}'$  (without labels).

**Remote Sensing:** We choose the Crop dataset (Crop) (Khosravi et al., 2018; Khosravi & Alavipanah, 2019). The optical features  $\mathbf{X}$  are used to predict the crop type, and the radar readings are used as reference dataset  $\mathbf{Z}'$  (without labels).

There is no overlapping instance among the training data (in space  $\mathcal{X}$ ), reference data (in space  $\mathcal{Z}$ ), and evaluation data (in space  $\mathcal{X}$ ).

## 5.2. Performance Evaluation

### 5.2.1. MODELS

It is difficult to directly compare the effectiveness of TAP against existing state-of-the-art neural network architectures since this work is the first to propose cross-modal learning from unlabeled data modalities. However, we can show the effectiveness of TAP by carefully examining the perfor-

mance difference between different variants of TAP.

The baseline is a single-modal neural network without TAP integration at all. However, even if TAP integration shows a performance advantage against traditional supervised learning models without unlabeled cross-modal information input, there are still several factors that might be contributing to the performance difference, which we list as follows and propose corresponding models to examine these factors.

1. **Factor:** Is there an actual performance difference between TAP integration and traditional supervised learning models?

**Model:** To show the performance advantage of TAP integration, we directly compare the simple multilayer perceptron (MLP) classifier and its TAP integration counterpart. This is the baseline model that will demonstrate the benefits of TAP integration. This is the **Baseline**, shown in the first graph of Fig. 3.

2. **Factor:** The increase in depth of the neural network might contribute to the performance difference.

**Model:** We propose a variant model that replaces the TAP with a feedforward neural network (FFN) that takes the output of the last layer as input, and the output of the FFN will be concatenated with the last layer's

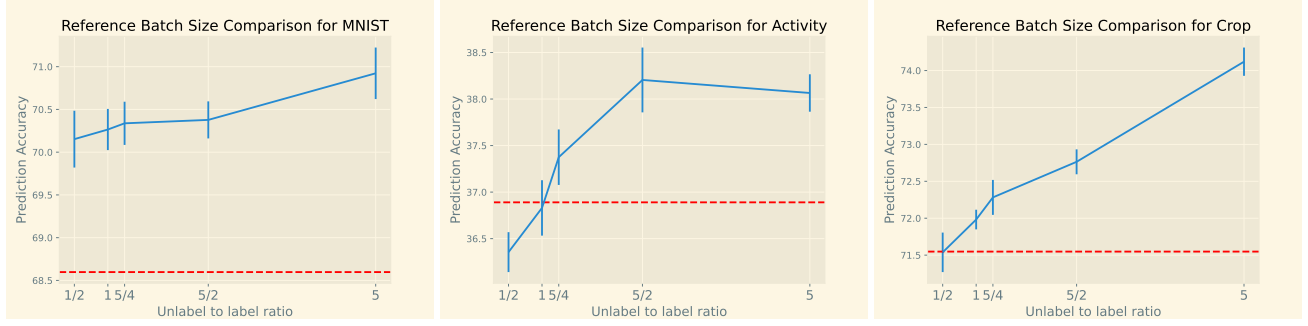


Figure 5. Reference batch size comparison on three real-world datasets.

output for the next layer. This is the **FFN**, shown in the second graph of Fig. 3.

- Factor:** The increase in parameter counts might be contributing to the performance difference, and the model is not learning the missing information from  $\mathbf{Z}'$ .

**Model:** To show that TAP indeed makes use of unlabeled modality  $\mathbf{Z}'$  rather than fitting a more complicated function on irrelevant data, we replace the cross-modality input  $\mathbf{Z}'$  with random noises with identical mean and standard deviation to  $\mathbf{Z}'$ . This is the **Control Group**, shown in the third graph of Fig. 3.

- Factor:** Batch training might contribute negatively to the model performance.

**Model:** We compare it with a TAP integration that uses all of  $\mathbf{Z}'$  throughout training and testing. This is **TAP w/o Batch**, shown in the last graph of Fig. 3.

### 5.2.2. RESULTS

The simulation results are shown in Fig. 4. The error bars are calculated over 20 Monte-Carlo simulations to reflect the statistical significance of the results. As we can see, there is a consistent performance hierarchy among all the benchmark models throughout all datasets in different areas. First, we see that TAP integration always leads to a performance improvement compared to the baseline classifier. Second, we see that the FFN variant shows no performance advantage against the baseline model, which rules out the factor that the increase in depth is responsible for performance improvement. Third, we observe the worst generalization performance across all benchmark models for the control group. This shows that feeding irrelevant information will exacerbate the generalization performance. Finally, we see that batch training and evaluation suffers from a slightly worse generalization performance than training directly with the whole reference dataset.

### 5.3. Reference Batch Size Comparison

To further evaluate the effect of batch training, we look at the performance of different reference batch sizes. The total number of reference data  $n'_z$  is five times of labeled data  $n_x$ . Fig. 5 shows the prediction accuracy with respect to “unlabel to label ratio”, which is defined as the reference batch size divided by  $n_x$ .

The performance of the baseline model is shown as the horizontal dotted line. We observe that the generalization performance improves as the reference batch size increases, even though the total number of reference data remains the same. This observation is consistent with the estimation error characterization in Theorem 4.3. In practice, this suggests one can increase the reference batch size as much as possible until the memory limit is reached.

## 6. Conclusion

In this paper, we adopt a novel perspective of supervised learning, where we aim to transfer knowledge from unlabeled cross-modal data to improve generalization on the primary modality. We formulate the problem from a missing information estimation perspective and provide an NW kernel regression interpretation of the problem. The formulation approximately leads to a cross-attention module in neural network integration. We name this module The Attention Patch (TAP). We implement the TAP integration on three real-world cross-modal datasets in different areas to show the performance advantage of TAP. We hope that this work can inspire a new perspective in knowledge transfer from the data level for neural networks, where seemingly unusable data can be utilized for improved generalization. There are also future directions that can potentially boost the method. For example, an approach that can efficiently store and reference the unlabeled modality will provide great benefits considering the wide availability of huge datasets. A principled framework for selecting relevant reference datasets will also be useful, just like in cross-modal learning



and semi-supervised learning.

## References

- Andrew, G., Arora, R., Bilmes, J., and Livescu, K. Deep canonical correlation analysis. In *International conference on machine learning*, pp. 1247–1255. PMLR, 2013.
- Baltrušaitis, T., Ahuja, C., and Morency, L.-P. Multimodal machine learning: A survey and taxonomy. *IEEE transactions on pattern analysis and machine intelligence*, 41(2):423–443, 2018.
- Berthelot, D., Carlini, N., Goodfellow, I., Papernot, N., Oliver, A., and Raffel, C. A. Mixmatch: A holistic approach to semi-supervised learning. *Advances in neural information processing systems*, 32, 2019.
- Blum, A. and Mitchell, T. Combining labeled and unlabeled data with co-training. In *Proceedings of the eleventh annual conference on Computational learning theory*, pp. 92–100, 1998.
- Bucak, S. S., Jin, R., and Jain, A. K. Multiple kernel learning for visual object recognition: A review. *IEEE Transactions on Pattern Analysis and Machine Intelligence*, 36(7):1354–1369, 2013.
- Castellano, G., Kessous, L., and Caridakis, G. Emotion recognition through multiple modalities: face, body gesture, speech. In *Affect and emotion in human-computer interaction*, pp. 92–103. Springer, 2008.
- Cha, J. Partial least squares. *Advanced methods of marketing research*, 407:52–78, 1994.
- Chen, X., Fang, H., Lin, T.-Y., Vedantam, R., Gupta, S., Dollár, P., and Zitnick, C. L. Microsoft coco captions: Data collection and evaluation server. *arXiv preprint arXiv:1504.00325*, 2015.
- Chen, Y., Zeng, Q., Ji, H., and Yang, Y. Skyformer: Re-model self-attention with gaussian kernel and nyström method. *Advances in Neural Information Processing Systems*, 34:2122–2135, 2021.
- Choromanski, K., Likhoshesterov, V., Dohan, D., Song, X., Gane, A., Sarlos, T., Hawkins, P., Davis, J., Mohiuddin, A., Kaiser, L., et al. Rethinking attention with performers. *arXiv preprint arXiv:2009.14794*, 2020.
- Deng, L. The mnist database of handwritten digit images for machine learning research. *IEEE Signal Processing Magazine*, 29(6):141–142, 2012.
- Devroye, L. and Wagner, T. The  $l_1$  convergence of kernel density estimates. *The Annals of Statistics*, 7(5):1136–1139, 1979.
- Dietterich, T. G. et al. Ensemble learning. *The handbook of brain theory and neural networks*, 2(1):110–125, 2002.
- Dópidio, I., Li, J., Marpu, P. R., Plaza, A., Dias, J. M. B., and Benediktsson, J. A. Semisupervised self-learning for hyperspectral image classification. *IEEE transactions on geoscience and remote sensing*, 51(7):4032–4044, 2013.
- Du, J., Ling, C. X., and Zhou, Z.-H. When does cotraining work in real data? *IEEE Transactions on Knowledge and Data Engineering*, 23(5):788–799, 2010.
- Evangelopoulos, G., Zlatintsi, A., Potamianos, A., Maragos, P., Rapantzikos, K., Skoumas, G., and Avrithis, Y. Multimodal saliency and fusion for movie summarization based on aural, visual, and textual attention. *IEEE Transactions on Multimedia*, 15(7):1553–1568, 2013.
- Feichtenhofer, C., Pinz, A., and Zisserman, A. Convolutional two-stream network fusion for video action recognition. In *Proceedings of the IEEE conference on computer vision and pattern recognition*, pp. 1933–1941, 2016.
- Frome, A., Corrado, G. S., Shlens, J., Bengio, S., Dean, J., Ranzato, M., and Mikolov, T. Devise: A deep visual-semantic embedding model. *Advances in neural information processing systems*, 26, 2013.
- Gehler, P. and Nowozin, S. On feature combination for multiclass object classification. In *2009 IEEE 12th International Conference on Computer Vision*, pp. 221–228. IEEE, 2009.
- Geladi, P. and Kowalski, B. R. Partial least-squares regression: a tutorial. *Analytica chimica acta*, 185:1–17, 1986.
- Gu, J., Cai, J., Joty, S. R., Niu, L., and Wang, G. Look, imagine and match: Improving textual-visual cross-modal retrieval with generative models. In *Proceedings of the IEEE conference on computer vision and pattern recognition*, pp. 7181–7189, 2018.
- Hardoon, D. R., Szedmak, S., and Shawe-Taylor, J. Canonical correlation analysis: An overview with application to learning methods. *Neural computation*, 16(12):2639–2664, 2004.
- Hong, C., Yu, J., Wan, J., Tao, D., and Wang, M. Multimodal deep autoencoder for human pose recovery. *IEEE transactions on image processing*, 24(12):5659–5670, 2015.
- Hong, D., Yokoya, N., Xia, G.-S., Chanussot, J., and Zhu, X. X. X-modalnet: A semi-supervised deep cross-modal network for classification of remote sensing data. *ISPRS Journal of Photogrammetry and Remote Sensing*, 167: 12–23, 2020.

- Jia, X., Jing, X.-Y., Zhu, X., Chen, S., Du, B., Cai, Z., He, Z., and Yue, D. Semi-supervised multi-view deep discriminant representation learning. *IEEE transactions on pattern analysis and machine intelligence*, 43(7):2496–2509, 2020.
- Jing, X.-Y., Hu, R.-M., Zhu, Y.-P., Wu, S.-S., Liang, C., and Yang, J.-Y. Intra-view and inter-view supervised correlation analysis for multi-view feature learning. In *Proceedings of the AAAI Conference on Artificial Intelligence*, volume 28, 2014.
- Karpathy, A. and Fei-Fei, L. Deep visual-semantic alignments for generating image descriptions. In *Proceedings of the IEEE conference on computer vision and pattern recognition*, pp. 3128–3137, 2015.
- Khosravi, I. and Alavipanah, S. K. A random forest-based framework for crop mapping using temporal, spectral, textural and polarimetric observations. *International Journal of Remote Sensing*, 40(18):7221–7251, 2019.
- Khosravi, I., Safari, A., and Homayouni, S. Msmd: maximum separability and minimum dependency feature selection for cropland classification from optical and radar data. *International Journal of Remote Sensing*, 39(8):2159–2176, 2018.
- Kiela, D. and Bottou, L. Learning image embeddings using convolutional neural networks for improved multi-modal semantics. In *Proceedings of the 2014 Conference on empirical methods in natural language processing (EMNLP)*, pp. 36–45, 2014.
- Kiritchenko, S. and Matwin, S. Email classification with co-training. In *Proceedings of the 2001 conference of the Centre for Advanced Studies on Collaborative research*, pp. 8, 2001.
- Kulkarni, G., Premraj, V., Ordonez, V., Dhar, S., Li, S., Choi, Y., Berg, A. C., and Berg, T. L. Babytalk: Understanding and generating simple image descriptions. *IEEE transactions on pattern analysis and machine intelligence*, 35(12):2891–2903, 2013.
- Lee, D.-H. et al. Pseudo-label: The simple and efficient semi-supervised learning method for deep neural networks. In *Workshop on challenges in representation learning, ICML*, volume 3, pp. 896, 2013.
- Li, C., Gao, S., Deng, C., Xie, D., and Liu, W. Cross-modal learning with adversarial samples. *Advances in neural information processing systems*, 32, 2019.
- Liang, J., Li, R., and Jin, Q. Semi-supervised multi-modal emotion recognition with cross-modal distribution matching. In *Proceedings of the 28th ACM International Conference on Multimedia*, pp. 2852–2861, 2020.
- Lin, D. and Tang, X. Inter-modality face recognition. In *European conference on computer vision*, pp. 13–26. Springer, 2006.
- Luo, S., Li, S., Cai, T., He, D., Peng, D., Zheng, S., Ke, G., Wang, L., and Liu, T.-Y. Stable, fast and accurate: Kernelized attention with relative positional encoding. *Advances in Neural Information Processing Systems*, 34:22795–22807, 2021.
- Mahasseni, B. and Todorovic, S. Regularizing long short term memory with 3d human-skeleton sequences for action recognition. In *Proceedings of the IEEE conference on computer vision and pattern recognition*, pp. 3054–3062, 2016.
- Mitchell, M., Dodge, J., Goyal, A., Yamaguchi, K., Stratos, K., Han, X., Mensch, A., Berg, A., Berg, T., and Daumé III, H. Midge: Generating image descriptions from computer vision detections. In *Proceedings of the 13th Conference of the European Chapter of the Association for Computational Linguistics*, pp. 747–756, 2012.
- Mohino-Herranz, I., Gil-Pita, R., Rosa-Zurera, M., and Seoane, F. Activity recognition using wearable physiological measurements: Selection of features from a comprehensive literature study. *Sensors*, 19(24), 2019.
- Nadaraya, E. A. On estimating regression. *Theory of Probability & Its Applications*, 9(1):141–142, 1964.
- Ngiam, J., Khosla, A., Kim, M., Nam, J., Lee, H., and Ng, A. Y. Multimodal deep learning. In *ICML*, 2011.
- Nie, F., Cai, G., and Li, X. Multi-view clustering and semi-supervised classification with adaptive neighbours. In *Thirty-first AAAI conference on artificial intelligence*, 2017a.
- Nie, F., Li, J., and Li, X. Convex multiview semi-supervised classification. *IEEE Transactions on Image Processing*, 26(12):5718–5729, 2017b.
- Nie, F., Tian, L., Wang, R., and Li, X. Multiview semi-supervised learning model for image classification. *IEEE Transactions on Knowledge and Data Engineering*, 32(12):2389–2400, 2019.
- Peng, H., Pappas, N., Yogatama, D., Schwartz, R., Smith, N., and Kong, L. Random feature attention. In *International Conference on Learning Representations*, 2020.
- Peng, Y. and Qi, J. Cm-gans: Cross-modal generative adversarial networks for common representation learning. *ACM Transactions on Multimedia Computing, Communications, and Applications (TOMM)*, 15(1):1–24, 2019.

- Peng, Y., Qi, J., Huang, X., and Yuan, Y. Ccl: Cross-modal correlation learning with multigrained fusion by hierarchical network. *IEEE Transactions on Multimedia*, 20(2):405–420, 2017.
- Ramirez, G. A., Baltrušaitis, T., and Morency, L.-P. Modeling latent discriminative dynamic of multi-dimensional affective signals. In *International Conference on Affective Computing and Intelligent Interaction*, pp. 396–406. Springer, 2011.
- Rosenberg, C., Hebert, M., and Schneidman, H. Semi-supervised self-training of object detection models. In *Applications of Computer Vision and the IEEE Workshop on Motion and Video Computing, IEEE Workshop on*, volume 1, pp. 29–36. IEEE Computer Society, 2005.
- Sagi, O. and Rokach, L. Ensemble learning: A survey. *Wiley Interdisciplinary Reviews: Data Mining and Knowledge Discovery*, 8(4):e1249, 2018.
- Sharma, A., Kumar, A., Daume, H., and Jacobs, D. W. Generalized multiview analysis: A discriminative latent space. In *2012 IEEE conference on computer vision and pattern recognition*, pp. 2160–2167. IEEE, 2012.
- Sohn, K., Shang, W., and Lee, H. Improved multimodal deep learning with variation of information. *Advances in neural information processing systems*, 27, 2014.
- Sohn, K., Berthelot, D., Carlini, N., Zhang, Z., Zhang, H., Raffel, C. A., Cubuk, E. D., Kurakin, A., and Li, C.-L. Fixmatch: Simplifying semi-supervised learning with consistency and confidence. *Advances in neural information processing systems*, 33:596–608, 2020.
- Tanha, J., Van Someren, M., and Afsarmanesh, H. Semi-supervised self-training for decision tree classifiers. *International Journal of Machine Learning and Cybernetics*, 8(1):355–370, 2017.
- Tenenbaum, J. B. and Freeman, W. T. Separating style and content with bilinear models. *Neural computation*, 12(6): 1247–1283, 2000.
- Triguero, I., García, S., and Herrera, F. Self-labeled techniques for semi-supervised learning: taxonomy, software and empirical study. *Knowledge and Information systems*, 42(2):245–284, 2015.
- Tsai, Y.-H. H., Bai, S., Liang, P. P., Kolter, J. Z., Morency, L.-P., and Salakhutdinov, R. Multimodal transformer for unaligned multimodal language sequences. In *Proceedings of the conference. Association for Computational Linguistics. Meeting*, volume 2019, pp. 6558. NIH Public Access, 2019.
- Van Engelen, J. E. and Hoos, H. H. A survey on semi-supervised learning. *Machine Learning*, 109(2):373–440, 2020.
- Vaswani, A., Shazeer, N., Parmar, N., Uszkoreit, J., Jones, L., Gomez, A. N., Kaiser, Ł., and Polosukhin, I. Attention is all you need. *Advances in neural information processing systems*, 30, 2017.
- Venugopalan, S., Xu, H., Donahue, J., Rohrbach, M., Mooney, R. J., and Saenko, K. Translating videos to natural language using deep recurrent neural networks. In *HLT-NAACL*, 2015.
- Wan, X. Co-training for cross-lingual sentiment classification. In *Proceedings of the Joint Conference of the 47th Annual Meeting of the ACL and the 4th International Joint Conference on Natural Language Processing of the AFNLP*, pp. 235–243, 2009.
- Wand, M. P. and Jones, M. C. *Kernel Smoothing*. CRC press, 1994.
- Wang, K., Yin, Q., Wang, W., Wu, S., and Wang, L. A comprehensive survey on cross-modal retrieval. *arXiv preprint arXiv:1607.06215*, 2016.
- Wang, Y. and Shahrampour, S. Orcca: Optimal randomized canonical correlation analysis. *IEEE Transactions on Neural Networks and Learning Systems*, 2021.
- Watson, G. S. Smooth regression analysis. *Sankhyā: The Indian Journal of Statistics, Series A*, pp. 359–372, 1964.
- Wu, Z., Wu, J., Cao, J., and Tao, D. Hysad: A semi-supervised hybrid shilling attack detector for trustworthy product recommendation. In *Proceedings of the 18th ACM SIGKDD international conference on Knowledge discovery and data mining*, pp. 985–993, 2012.
- Xie, Q., Luong, M.-T., Hovy, E., and Le, Q. V. Self-training with noisy student improves imagenet classification. In *Proceedings of the IEEE/CVF conference on computer vision and pattern recognition*, pp. 10687–10698, 2020.
- Xiong, Y., Zeng, Z., Chakraborty, R., Tan, M., Fung, G., Li, Y., and Singh, V. Nyströmformer: A nyström-based algorithm for approximating self-attention. In *Proceedings of the AAAI Conference on Artificial Intelligence*, volume 35, pp. 14138–14148, 2021.
- Xu, R., Xiong, C., Chen, W., and Corso, J. Jointly modeling deep video and compositional text to bridge vision and language in a unified framework. In *Proceedings of the AAAI Conference on Artificial Intelligence*, volume 29, 2015.

- Yarowsky, D. Unsupervised word sense disambiguation rivaling supervised methods. In *33rd annual meeting of the association for computational linguistics*, pp. 189–196, 1995.
- Yu, E., Sun, J., Li, J., Chang, X., Han, X.-H., and Hauptmann, A. G. Adaptive semi-supervised feature selection for cross-modal retrieval. *IEEE Transactions on Multimedia*, 21(5):1276–1288, 2018.
- Zhang, L., Ma, B., He, J., Li, G., Huang, Q., and Tian, Q. Adaptively unified semi-supervised learning for cross-modal retrieval. In *IJCAI*, pp. 3406–3412, 2017.
- Zhang, S., Chen, M., Chen, J., Li, Y.-F., Wu, Y., Li, M., and Zhu, C. Combining cross-modal knowledge transfer and semi-supervised learning for speech emotion recognition. *Knowledge-Based Systems*, 229:107340, 2021.
- Zhu, X. J. Semi-supervised learning literature survey. *Technical Report TR 1530*, 2005.
- Zoph, B., Ghiasi, G., Lin, T.-Y., Cui, Y., Liu, H., Cubuk, E. D., and Le, Q. Rethinking pre-training and self-training. *Advances in neural information processing systems*, 33:3833–3845, 2020.

## A. Appendix

We first provide the experimental details for reproducibility. The code is also provided in the supplementary material. Then, we introduce a simple lemma that shows multivariate kernel density estimator is a consistent density estimator that converges in probability. The last section is the proof of Theorem 4.3.

### A.1. Experimental Details

#### A.1.1. DATASET

##### Dataset Description:

MNIST dataset is a well-known dataset with 784 pixel value features. We crop the upper half of images as the primary modality, which corresponds to the first 392 features in the dataset, and the rest 392 features form the lower images. In this case, we know for sure that the two modalities are located in different spaces and carry complementary information.

Activity dataset is an activity prediction dataset that predicts the status of a person through wearable physiological measurements. There are 151 features for Thoracic Electrical Bioimpedance (TEB) readings and 208 features for Electrodermal Activity (EDA) readings including 104 for left arm readings and 104 for right arm readings. The objective is to predict the activity that the subject is currently going through, including neutral, mental, emotional, and physical activities.

Crop dataset is a crop type prediction dataset that predicts the type of crop a land is growing using satellite and radar readings. There are 76 optical features collected with RapidEye satellites and 98 radar features collected with the Unmanned Aerial Vehicle Synthetic Aperture Radar system. The labels contain seven crop types, including Corn, Peas, Canola, Soybeans, Oats, Wheat, and Broadleaf.

##### Data Preprocessing:

Just like in semi-supervised learning, the motivation behind utilizing unlabeled data points is the limited availability of labeled data. So, we randomly sample 200 data points in the primary modality to serve as the training data for each dataset. We further randomly sample 1000 data points in the secondary modality to serve as the cross-modal reference data. For MNIST, it means 200 upper images as primary modality training data and 1000 lower images as reference data. All the remaining data points will be the evaluation data.

#### A.1.2. PERFORMANCE EVALUATION

##### Parameter Setting:

In the performance evaluation, the reference batch size for TAP is chosen as 250, which is 1.25 times the training data. The training data batch size is set to 100. As shown in the reference batch size comparison, 250 is not the best-performing choice, but it always yields better generalization accuracy on these three datasets.

The backbone neural network structure for all three datasets is a two-hidden-layer neural network with 64 hidden neurons at each layer. The activation function is ReLU, with a dropout rate of 0.5. Layer normalization is implemented after each hidden layer. TAP is integrated between the two hidden layers. For TAP, TAP w/o Batch, FNN, and Control Group, the second hidden layer still has 64 neurons, except the linear layer takes input from  $\mathbb{R}^{128}$  and outputs  $\mathbb{R}^{64}$ .

The hidden dimension in TAP is also set to 64, and the output is also 64. FNN replaces the attention module in TAP with a linear layer from  $\mathbb{R}^{64}$  to  $\mathbb{R}^{64}$ . Layer normalization is also implemented in TAP (including TAP w/o Batch and Control Group) and FNN as well. The normalization parameter in the attention module of TAP is set to  $\sqrt{d}(n'_z/m)^{-1/d}$  such that it follows the bandwidth Assumption 4.1 while being close to the general recommended normalization constant  $\sqrt{d}$ .

At each Monte-Carlo Simulation, the set of training data, reference data, and evaluation data are shuffled while keeping the amount the same. The control group also generates a new set of random reference data at each Monte-Carlo simulation.

##### Network Training:

All benchmark variant models share a similar backbone structure, therefore the training process is also similar. All models are trained with the cross-entropy loss using the Adam optimizer with a fixed learning rate of 0.0001. All models are trained for 1000 epochs (8000 in the Crop dataset) except for TAP. Since TAP updates the model several times within one epoch, the total training epoch for TAP is reduced to  $1000/m$ , where  $m$  is the number of reference batches. For example, in the



case of performance evaluation where the reference batch size is 250, there are four batches of reference data, and the total training epoch is 250 for TAP. The prediction accuracy is calculated as the lowest five-moving-average of validation accuracy throughout the training process, which is a common practice in neural network performance evaluation.

The batch evaluation of TAP is done by having each batch of reference data generate a prediction class, and finding the majority vote among all batches just like ensemble methods.

### A.1.3. REFERENCE BATCH SIZE COMPARISON

The experimental settings in this section of the simulation are pretty much identical to the previous section. The reference batch sizes are chosen as 100, 200, 250, 500, 1000, which corresponds to the unlabeled to labeled ratio  $1/2, 1, 5/4, 5/2, 5$ . The corresponding training epochs are 100, 200, 250, 500, 1000 respectively. For the Crop dataset, all training epochs are multiplied by 8 since it takes longer to train.

## A.2. Lemma

**Lemma A.1.** *Under Assumptions 4.1 and 4.2, a kernel density estimator*

$$\hat{p}(\mathbf{x}) = \frac{1}{n} \sum_{i=1}^n k_{\mathbf{H}}(\mathbf{x}, \mathbf{x}'_i), \quad (15)$$

is consistent, i.e., it converges in probability to the true density function  $p(\mathbf{x})$ ,

$$\hat{p}(\mathbf{x}) \xrightarrow{p} p(\mathbf{x}). \quad (16)$$

This is a well-known result that can be found in existing literature (Devroye & Wagner, 1979).

## A.3. Proof of Theorem 4.3

Throughout the proof, all integrals are Riemann integral  $\int_{\mathbb{R}^d}$ , and we omit the subscript for simplicity. Since we are strictly talking about shift-invariant kernels, we will use  $k_{\mathbf{H}}(\mathbf{x} - \mathbf{x}'_i)$  to represent an isotropic kernel function with bandwidth  $\mathbf{H} = h\mathbf{I}$ , where  $k_{\mathbf{H}}(\mathbf{x} - \mathbf{x}'_i) = \frac{1}{|\mathbf{H}|} k(\frac{\mathbf{x} - \mathbf{x}'_i}{|\mathbf{H}|})$ . The determinant of the bandwidth matrix by definition is  $|\mathbf{H}| = h^d$ .

Consider the  $j$ -th element in  $\mathbf{z}'_i$ , where we simply write as  $z^{(j)}$ . Then, we have the following

$$\begin{aligned} \hat{f}^{(j)}(\mathbf{x}) &= \frac{\frac{1}{n} \sum_{i=1}^n k_{\mathbf{H}}(\mathbf{x} - \mathbf{x}'_i) z^{(j)}}{\hat{p}(\mathbf{x})} \\ &= \frac{\frac{1}{n} \sum_{i=1}^n k_{\mathbf{H}}(\mathbf{x} - \mathbf{x}'_i) (f^{(j)}(\mathbf{x}) + f^{(j)}(\mathbf{x}'_i) - f^{(j)}(\mathbf{x}) + \epsilon_i^{(j)})}{\hat{p}(\mathbf{x})} \\ &= f^{(j)}(\mathbf{x}) + \frac{\frac{1}{n} \sum_{i=1}^n k_{\mathbf{H}}(\mathbf{x} - \mathbf{x}'_i) (f^{(j)}(\mathbf{x}'_i) - f^{(j)}(\mathbf{x}))}{\hat{p}(\mathbf{x})} + \frac{\frac{1}{n} \sum_{i=1}^n k_{\mathbf{H}}(\mathbf{x} - \mathbf{x}'_i) \epsilon_i^{(j)}}{\hat{p}(\mathbf{x})} \\ &\triangleq f^{(j)}(\mathbf{x}) + \frac{B(\mathbf{x})}{\hat{p}(\mathbf{x})} + \frac{V(\mathbf{x})}{\hat{p}(\mathbf{x})}, \end{aligned} \quad (17)$$

where we theoretically characterize the properties of  $B(\mathbf{x})$  and  $V(\mathbf{x})$ . We refer to a single term in the summation  $B(\mathbf{x})$  and  $V(\mathbf{x})$  as  $b_i(\mathbf{x})$  and  $v_i(\mathbf{x})$ , and the subscripts will be omitted from now on for simplicity.

We first look at the term  $v(\mathbf{x})$ , and it is easy to see that  $\mathbb{E}[v(\mathbf{x})] = 0$  due to our assumption on the noise term  $\epsilon$ . For the

variance, we have the following asymptotic equality

$$\begin{aligned}
 \mathbb{E}[|\mathbf{H}|v^2(\mathbf{x})] &= \mathbb{E}[\epsilon^2]|\mathbf{H}| \int k_{\mathbf{H}}^2(\mathbf{x} - \mathbf{y})p(\mathbf{y})d\mathbf{y} \\
 &= \frac{\sigma^2}{|\mathbf{H}|} \int k^2\left(\frac{\mathbf{x} - \mathbf{y}}{|\mathbf{H}|}\right)p(\mathbf{y})d\mathbf{y} \\
 &= \sigma^2 \int k^2(\mathbf{z})p(\mathbf{x} - |\mathbf{H}|\mathbf{z})d\mathbf{z} \\
 &= \sigma^2 \int k^2(\mathbf{z})(p(\mathbf{x}) + o(1))d\mathbf{z} \\
 &\asymp R(k)p(\mathbf{x})\sigma^2,
 \end{aligned} \tag{18}$$

where the last line follows from omitting the higher order term. Since  $V(\mathbf{x})$  is the mean of random variables  $v(\mathbf{x})$ , we can apply the central limit theorem to show that

$$\sqrt{nh^d}V(\mathbf{x}) \xrightarrow{d} \mathcal{N}(0, R(k)p(\mathbf{x})\sigma^2). \tag{19}$$

Since  $\hat{p}(\mathbf{x}) \xrightarrow{p} p(\mathbf{x})$  following Lemma A.1, we can make the claim following Slutsky's theorem

$$\frac{\sqrt{nh^d}V(\mathbf{x})}{\hat{p}(\mathbf{x})} \xrightarrow{d} \mathcal{N}(0, \frac{R(k)\sigma^2}{p(\mathbf{x})}). \tag{20}$$

Then, let us look at the term  $b(\mathbf{x})$ . We have the following

$$\begin{aligned}
 &\mathbb{E}[b(\mathbf{x})] \\
 &= \frac{1}{|\mathbf{H}|} \mathbb{E}\left[k\left(\frac{\mathbf{x}'_i - \mathbf{x}}{|\mathbf{H}|}\right)(f^{(j)}(\mathbf{x}'_i) - f^{(j)}(\mathbf{x}))\right] \\
 &= \frac{1}{|\mathbf{H}|} \int k\left(\frac{\mathbf{y} - \mathbf{x}}{|\mathbf{H}|}\right)(f^{(j)}(\mathbf{y}) - f^{(j)}(\mathbf{x}))p(\mathbf{y})d\mathbf{y} \\
 &= \int k(\mathbf{z})(f^{(j)}(\mathbf{x} + |\mathbf{H}|\mathbf{z}) - f^{(j)}(\mathbf{x}))p(\mathbf{x} + |\mathbf{H}|\mathbf{z})d\mathbf{z} \\
 &\asymp \int k(\mathbf{z})\left((|\mathbf{H}|\mathbf{z})^\top \nabla f^{(j)}(\mathbf{x}) + \frac{1}{2}(|\mathbf{H}|\mathbf{z})^\top \nabla^2 f^{(j)}(\mathbf{x})(|\mathbf{H}|\mathbf{z})\right)\left(p(\mathbf{x}) + (|\mathbf{H}|\mathbf{z})^\top \nabla p(\mathbf{x})\right)d\mathbf{z} \\
 &\asymp |\mathbf{H}| \int k(\mathbf{z})\mathbf{z}^\top \nabla f^{(j)}(\mathbf{x})p(\mathbf{x})d\mathbf{z} + |\mathbf{H}|^2 \text{Tr} \left[ \int k(\mathbf{z})p(\mathbf{x}) \frac{1}{2} \nabla^2 f^{(j)}(\mathbf{x}) \mathbf{z}\mathbf{z}^\top d\mathbf{z} \right] \\
 &\quad + |\mathbf{H}|^2 \text{Tr} \left[ \int k(\mathbf{z}) \nabla f^{(j)}(\mathbf{x}) \nabla p(\mathbf{x})^\top \mathbf{z}\mathbf{z}^\top d\mathbf{z} \right] \\
 &= |\mathbf{H}|^2 \mu_2(k) \left( \frac{1}{2} p(\mathbf{x}) \text{Tr} \left[ \nabla^2 f^{(j)}(\mathbf{x}) \right] + \text{Tr} \left[ \nabla f^{(j)}(\mathbf{x}) \nabla p(\mathbf{x})^\top \right] \right) \\
 &\triangleq |\mathbf{H}|^2 \mu_2(k) \Psi^{(j)}(\mathbf{x}) = h^{2d} \mu_2(k) \Psi^{(j)}(\mathbf{x}).
 \end{aligned} \tag{21}$$

Any term that is  $o(|\mathbf{H}|^2)$  is omitted as it asymptotically vanishes.

For the term  $\mathbb{E}[b^2(\mathbf{x})]$ , we use a similar expansion by omitting terms of  $o(|\mathbf{H}|^2)$  as follows

$$\begin{aligned}
 \mathbb{E}[b^2(\mathbf{x})] &= \frac{1}{|\mathbf{H}|^2} \mathbb{E} \left[ k^2 \left( \frac{\mathbf{x}'_i - \mathbf{x}}{|\mathbf{H}|} \right) (f^{(j)}(\mathbf{x}'_i) - f^{(j)}(\mathbf{x}))^2 \right] \\
 &= \frac{1}{|\mathbf{H}|^2} \int k^2 \left( \frac{\mathbf{y} - \mathbf{x}}{|\mathbf{H}|} \right) (f^{(j)}(\mathbf{y}) - f^{(j)}(\mathbf{x}))^2 p(\mathbf{y}) d\mathbf{y} \\
 &= \frac{1}{|\mathbf{H}|} \int k^2(\mathbf{z}) (f^{(j)}(\mathbf{x} + |\mathbf{H}|\mathbf{z}) - f^{(j)}(\mathbf{x}))^2 p(\mathbf{x} + |\mathbf{H}|\mathbf{z}) d\mathbf{z} \\
 &\asymp \frac{1}{|\mathbf{H}|} \int k^2(\mathbf{z}) ((|\mathbf{H}|\mathbf{z})^\top \nabla f^{(j)}(\mathbf{x}))^2 p(\mathbf{x}) d\mathbf{z} \\
 &= O \left( |\mathbf{H}| \nabla f^{(j)}(\mathbf{x})^\top \nabla f^{(j)}(\mathbf{x}) p(\mathbf{x}) \mu_2(k) \right).
 \end{aligned} \tag{22}$$

This suggests that the variance of  $b(\mathbf{x})$  is of a higher order than the variance of  $\sqrt{|\mathbf{H}|}v(\mathbf{x})$ . Thus, we know

$$\sqrt{nh^d} (B(\mathbf{x}) - h^{2d} \mu_2(k) \Psi^{(j)}(\mathbf{x})) \xrightarrow{p} 0. \tag{23}$$

Combining with the convergence in probability for density estimator  $\hat{p}(\mathbf{x})$ , we have

$$\sqrt{nh^d} \left( \frac{B(\mathbf{x})}{\hat{p}(\mathbf{x})} - \frac{h^{2d} \mu_2(k) \Psi^{(j)}(\mathbf{x})}{p(\mathbf{x})} \right) \xrightarrow{p} 0. \tag{24}$$

Finally, we conclude that

$$\begin{aligned}
 &\sqrt{nh^d} \left( \mathbf{e}(\mathbf{x}) - \frac{h^{2d} \mu_2(k) \Psi(\mathbf{x})}{p(\mathbf{x})} \right) \\
 &= \sqrt{nh^d} \left( \frac{\mathbf{B}(\mathbf{x})}{\hat{p}(\mathbf{x})} - \frac{h^{2d} \mu_2(k) \Psi(\mathbf{x})}{p(\mathbf{x})} + \frac{\mathbf{V}(\mathbf{x})}{\hat{p}(\mathbf{x})} \right) \xrightarrow{d} \mathcal{N}(\mathbf{0}, \frac{R(k)\sigma^2}{p(\mathbf{x})} \mathbf{I}),
 \end{aligned} \tag{25}$$

where  $\mathbf{B}(\mathbf{x})$  and  $\mathbf{V}(\mathbf{x})$  are the vectorization of  $B(\mathbf{x})$  and  $V(\mathbf{x})$ , respectively.

The proof is complete.